ACCELERATED PUBLICATION

Binding of phosphatidylinositol 3,4,5-trisphosphate to the pleckstrin homology domain of protein kinase B induces a conformational change

Christine C. MILBURN*, Maria DEAK†, Sharon M. KELLY‡, Nick C. PRICE‡, Dario R. ALESSI† and Daan M. F. VAN AALTEN*[1]

*Division of Biological Chemistry and Molecular Microbiology, School of Life Sciences, University of Dundee, Dundee DD1 5EH, U.K., †MRC Protein Phosphorylation Unit, School of Life Sciences, University of Dundee, Dundee DD1 5EH, U.K., and ‡Joseph Black Building, Glasgow University, Glasgow G12 8QQ, U.K.

Protein kinase B (PKB/Akt) is a key regulator of cell growth, proliferation and metabolism. It possesses an N-terminal pleckstrin homology (PH) domain that interacts with equal affinity with the second messengers PtdIns(3,4,5)P_3 and PtdIns(3,4)P_2, generated through insulin and growth factor-mediated activation of phosphoinositide 3-kinase (PI3K). The binding of PKB to PtdIns(3,4,5)P_3/PtdIns(3,4)P_2 recruits PKB from the cytosol to the plasma membrane and is also thought to induce a conformational change that converts PKB into a substrate that can be activated by the phosphoinositide-dependent kinase 1 (PDK1). In this study we describe two high-resolution crystal structures of the PH domain of PKBα in a noncomplexed form and compare this to a new atomic resolution (0.98 Å, where 1 Å = 0.1 nm) structure of the PH domain of PKBα complexed to Ins(1,3,4,5)P_4, the head group of PtdIns(3,4,5)P_3. Remarkably, in contrast to all other PH domains crystallized so far, our data suggest that binding of Ins(1,3,4,5)P_4 to the PH domain of PKB, induces a large conformational change. This is characterized by marked changes in certain residues making up the phosphoinositide-binding site, formation of a short α-helix in variable loop 2, and a movement of variable loop 3 away from the lipid-binding site. Solution studies with CD also provided evidence of conformational changes taking place upon binding of Ins(1,3,4,5)P_4 to the PH domain of PKB. Our data provides the first structural insight into the mechanism by which the interaction of PKB with PtdIns(3,4,5)P_3/PtdIns(3,4)P_2 induces conformational changes that could enable PKB to be activated by PDK1.

Key words: circular dichroism (CD), crystallography, PDK1, phosphoinositide 3-kinase (PI3K).

INTRODUCTION

Stimulation of cells with growth factors or insulin leads to the recruitment of phosphoinositide 3-kinase (PI3K) to the plasma membrane where it phosphorylates PtdIns(4,5)P_2 at the D3 hydroxy group of the inositol ring to generate PtdIns(3,4,5)P_3, which can then be converted to PtdIns(3,4)P_2 through the actions of the Src homology domain 2-containing inositol 5-phosphatases [1]. Recent work has established that PtdIns(3,4,5)P_3, and perhaps PtdIns(3,4)P_2, function as key second messengers mediating many of the survival and metabolic responses controlled by insulin and growth factors [2,3,4]. It is well established that one of the major mechanisms by which PtdIns(3,4,5)P_3 exerts its physiological effects, is by interacting with proteins possessing pleckstrin homology (PH) domains [5,6]. One such PtdIns(3,4,5)P_3/PtdIns(3,4)P_2 effector protein is the serine/threonine protein kinase termed protein kinase B (PKB, also known as Akt), which phosphorylates numerous regulatory proteins to enhance cell survival, proliferation and mediates metabolic responses [7,8]. In a significant number of cancer-cell types, PKB activity is elevated and this is thought to contribute to the enhanced ability of these cells to survive and proliferate (reviewed in [9,10,11]).

PKB possesses an N-terminal PH domain which binds PtdIns(3,4,5)P_3 and PtdIns(3,4)P_2 with similar affinity, but does not interact with PtdIns(4,5)P_2, PtdIns3P or PtdIns4P [12,13]. Following stimulation of cells with agonists that activate PI3K, PKB is recruited to the plasma membrane by virtue of its interaction with PtdIns(3,4,5)P_3 and/or PtdIns(3,4)P_2 [14,15]. This interaction does not activate PKB directly but instead brings it into the vicinity of the phosphoinositide-dependent kinase 1 (PDK1), which activates PKB by phosphorylating the activation loop [16]. PKB is also phosphorylated at a C-terminal non-catalytic residue termed the hydrophobic motif, at the plasma membrane by a distinct uncharacterized protein kinase [16]. Phosphorylation of PKB at its activation loop is the key activating phosphorylation step, but phosphorylation of the hydrophobic motif is required for maximal activation of PKB [17]. PDK1, like PKB, possesses a PH domain that interacts with PtdIns(3,4,5)P_3 and PtdIns(3,4)P_2 and it is thought that the binding of both PKB and PDK1 to these 3-phosphoinositides is a major driving force for bringing these enzymes together at the plasma membrane in growth factor- and insulin-stimulated cells. However, although this co-localisation is an important determinant in enabling PDK1 to phosphorylate PKB, the binding of PKB to phospholipids is also postulated to induce a conformational change in PKB, exposing the activation loop, thereby permitting it to be phosphorylated by PDK1. The evidence for this is based upon the observation that in the absence of 3-phosphoinositides, PDK1 is unable to phosphorylate wild-type PKB under conditions where it is able to efficiently phosphorylate a mutant form of PKB that lacks its PH domain, termed ΔPH-PKB [18,19]. Moreover, artificially promoting the interaction of PDK1 with wild-type PKB and ΔPH-PKB by the attachment of a high affinity PDK1 interaction motif to these enzymes, was sufficient to induce maximal phosphorylation of the activation loop in ΔPH-PKB, but not in wild-type PKB in unstimulated cells [20]. More recently Calleja et al. [21] have presented elegant evidence, employing fluorescence lifetime imaging microscopy, that recruitment of PKB to

Abbreviations used: diC$_8$, dioctanoyl; GST, glutathione S-transferase; PDK1, phosphoinositide-dependent kinase 1; PEG, poly(ethylene glycol); PH, pleckstrin homology; PKB, protein kinase B; PI3K, phosphoinositide 3-kinase; RMSD, root-mean-square deviation.

[1] To whom correspondence should be addressed (e-mail dava@davapc1.bioch.dundee.ac.uk).

the plasma membrane in platelet-derived growth factor (PDGF)-stimulated NIH3T3 cells resulted in a marked conformational change in PKB. Unfortunately, although the structures of the isolated PH domain of PKB complexed with Ins(1,3,4,5)P_4 [the head group of PtdIns(3,4,5)P_3] [22] and the isolated kinase domain of inactive [23] and active [24] PKB have recently been reported, these structures do not reveal how PtdIns(3,4,5)P_3 binding to PKB could induce a conformational change or in which region of PKB this conformational change takes place.

In this study we have analysed two crystal structures of the PH domain of PKBα (PKBαPH) in an apo state, one with an empty lipid-binding site (1.65 Å resolution) and the other with one sulphate molecule in this pocket (1.25 Å resolution). In addition we have also determined an atomic resolution (0.98 Å) structure of PKBαPH in complex with Ins(1,3,4,5)P_4. The data present structural evidence that binding of PtdIns(3,4,5)P_3 to PKB induces a conformational change within the PH domain, a conclusion which we also support using CD spectroscopy.

EXPERIMENTAL PROCEDURES

Materials

The phosphoinositides used in this study were dipalmitoyl derivatives obtained from Cell Signals (Columbus, OH, U.S.A.). pGEX4T-1 vector, thrombin protease and glutathione–Sepharose were from Amersham Biosciences (Little Chalfont, Bucks., U.K.). Protease inhibitor tablets were from Roche, benzamidine–agarose was from Sigma, and VivaSpin concentrators were from Vivascience (Hannover, Germany).

Expression of PKBαPH

The cloning, expression and crystallization methods of PKBαPH protein were performed as described previously [22]. Briefly, the PH domain of human PKBα (residues 1–123) was expressed in BL21 *Escherichia coli* cells as a glutathione S-transferase (GST)-fusion protein from a pGEX4T-1 plasmid. After expression, PKBαPH was affinity purified on glutathione–Sepharose, the GST-tag was removed by thrombin digestion and the PKBαPH purified on a Superdex 75 26/60 gel filtration column (Amersham Biosciences). PKBαPH purified in this manner was homogeneous, as verified by SDS/PAGE and MS.

Crystallization of PKBαPH

Monoclinic (C2) crystals (Table 1) of apo PKBαPH, diffracting to 1.65 Å, were grown by incubating 8.5 mg/ml PKBαPH with a 10-fold molar excess of 4-sulphophthalic acid for 30 min on ice. Crystallization was achieved using a mother liquor containing 30 % PEG [poly(ethylene glycol)] 4000, 0.25 M sodium acetate, 0.1 M Tris/HCl (pH 8.5), with the addition of 0.25 μl of 30 % poly(propylene glycol) 400 to the 2 μl drop. Crystals appeared after 2 days, growing to $0.2 \times 0.2 \times 0.3$ mm over 4 days. The crystals were frozen in a nitrogen gas stream without further cryo-protection. The PKBαPH-sulphate complex monoclinic (C2) crystals (Table 1), diffracting to 1.25 Å, were grown after incubation of 8.5 mg/ml PKBαPH with a 10-fold molar excess of dioctanoyl (diC_8)-PtdIns(3,4,5)P_3 for 30 min on ice at 20 °C from a mother liquor containing 0.2 M ammonium sulphate, 0.1 M Tris/HCl (pH 8.5). Crystals reached their maximum size of $0.2 \times 0.2 \times 0.3$ mm over 4 weeks. Crystals were frozen in a nitrogen gas stream after being soaked in 10 % 2-methyl-2,4-pentanediol for 30 s. The crystals for the PKBαPH complex with Ins(1,3,4,5)P_4 were produced by incubating 8.5 mg/ml PKBαPH with a 10:1 molar excess of ligand for 30 min on ice. The complex was crystallized using the hanging drop vapour diffusion method with a mother liquor containing 0.25 M ammonium acetate, 30 % PEG 4000, 0.1 M sodium acetate (pH 4.6). Monoclinic crystals (Table 1) appeared after 2 days, growing to approximately $0.2 \times 0.2 \times 0.3$ mm after four days. Crystals were frozen in a nitrogen gas stream after being soaked in 10 % 2-methyl-2,4-pentanediol for 30 s. The final pH of the crystallization drop containing protein for the PKBαPH apo structure and the PKBαPH-Ins(1,3,4,5)P_4 complex was pH 7.0 and pH 6.2, respectively.

Table 1 Details of data collection and structure refinement of the PKBαPH-Ins(1,3,4,5)P_4, apo PKBαPH and PKBαPH-sulphate data sets

Values in parentheses are for the highest resolution shell. All measured data were included in structure refinement. $\langle B \rangle$, average *B*-factor

	Structure		
	Ins(1,3,4,5)P_4	Apo	Sulphate
Wavelength (Å)	0.920177	0.97949	0.933
Space group	C2	C2	C2
Unit cell (Å)	$a = 82.90$ $b = 34.39$ $c = 44.29$ $\beta = 115.29°$	$a = 84.06$ $b = 33.80$ $c = 42.07$ $\beta = 119.48°$	$a = 83.73$ $b = 33.96$ $c = 42.28$ $\beta = 119.85°$
Resolution (Å)	15–0.98(1.02–0.98)	30–1.65(1.71–1.65)	15–1.25(1.29–1.25)
Observed reflections	203 345	37 427	119 529
Unique reflections	60 005	12 409	27 697
Redundancy	3.4(3.2)	3.0(2.7)	4.3(2.4)
Completeness (%)	93.2(92.9)	98.7(97.2)	96.2(74.6)
R_{merge}	0.064(0.557)	0.048(0.409)	0.073(0.394)
I/ sigma *I*	19.3(2.8)	24.3(4.1)	21.5(2.7)
R_{free} reflections	2429	601	902
R_{cryst}	0.154	0.203	0.173
R_{free}	0.179	0.239	0.226
Number of atoms			
Protein	987	998	956
Water	148	131	62
Ligand	28	–	5
Wilson *B* (Å^2)	14.7	21.8	26.7
$\langle B \rangle$ protein (Å^2)	13.6	20.7	26.3
$\langle B \rangle$ water (Å^2)	22.1	30.6	31.9
$\langle B \rangle$ ligand (Å^2)	8.7	–	24.7
RMSD from ideal geometry			
Bond lengths (Å)	0.013	0.006	0.006
Bond angles (°)	2.23	1.31	1.62
Main chain B (Å^2)	3.4	1.9	3.1

Data collection, structure solution, and refinement

Data on the PKBαPH apo crystal were collected at the Daresbury Synchrotron Radiation Facility (Warrington, Chesire, U.K.) on Station 14.2 using an ADSC Q4 CCD detector. Data on the PKBαPH-sulphate complex were collected at the European Synchrotron Radiation Facility (Grenoble, France) beamline ID14-EH2. Data on the PKBαPH-Ins(1,3,4,5)P_4 complex were collected at the European Synchrotron Radiation Facility beam line ID29, using an ADSC Q210 CCD detector. In each case the temperature of the crystals was maintained at 100 K using a

nitrogen cryostream. Data were processed using the HKL package [25]. The statistics for each dataset are shown in Table 1.

The 1.65 Å apo PKBαPH structure was solved by molecular replacement with AMoRe program [26], using the previously characterized selenomethionine-PKBαPH-Ins(1,3,4,5)P_4 complex structure (Protein Database 1H10) [22] as a search model against 8–4 Å data. A distinct solution with an *R*-factor of 0.36 and a correlation coefficient of 0.61 was found. The resulting model phases were used as input for warpNtrace [27], which was able to build 94 out of the 123 possible residues. Iterative model building in O [28], together with refinement in CNS [29], resulted in a final model with $R = 0.203$ ($R_{free} = 0.239$), which included residues 3–120. The statistics for this structure are in Table 1.

The 1.25 Å PKBαPH-sulphate complex was solved by molecular replacement with AMoRe [26], using the 1.65 Å PKBαPH apo structure described above as a search model, against 8–4 Å data. A solution with an *R*-factor of 0.42 and a correlation coefficient of 0.47 was found. The resulting model was used as input for CNS rigid body refinement and simulated annealing. Initial maps were calculated and showed continuous density for residues 3–42 and 50–120. Iterative model building in O [28], together with refinement in CNS [29], resulted in a model with $R = 0.275$ ($R_{free} = 0.288$), which included residues 3–120. Refinement was then continued with SHELX-97 [30], employing atomic anisotropic B-factors. The electron density corresponding to the sulphate molecule was interpreted in the third round of refinement. As a final step, riding hydrogens were included in the refinement, resulting in the final model with $R = 0.173$ ($R_{free} = 0.226$) which encompassed residues 1–42 and 48–120. The statistics for this structure are in Table 1.

The atomic resolution structure of PKBαPH domain bound to Ins(1,3,4,5)P_4 was initially refined using one round of CNS [29], and data to 1.4 Å. The first round of refinement included the use of rigid body refinement and simulated annealing and started with the structure of the previously characterized selenomethionine-PKBαPH-Ins(1,3,4,5)P_4-complex structure (PDB 1H10) [22], with the ligand and water molecules removed. Initial maps showed continuous density for residues 31–117. Refinement was then continued with SHELX-97 program [30] against the full resolution (0.98 Å), employing atomic anisotropic *B*-factors and, as a final step, riding hydrogens, resulting in the final model with $R = 0.155$ ($R_{free} = 0.193$) which encompassed residues 1–117 and an Ins(1,3,4,5)P_4 molecule. The statistics for this structure are in Table 1.

Importantly, it should be noted that all three PKBαPH structures described in this study were crystallized within the same space group (C2) with similar units cell dimensions (Table 1), and an analysis of crystal contacts between symmetry related molecules for each structure using the WHAT IF program [31], showed that the majority of crystal contacts have been conserved. It is thus unlikely that conformational changes discussed here are due to packing artefacts.

Figures were generated using the PyMOL (http://www.pymol.org) and GRASP [32] programs.

CD measurements

CD spectra were recorded on a Jasco J600 spectropolarimeter at 20 °C using cells of path length 0.5 cm and 0.02 cm in the near UV and far UV regions respectively. The protein concentrations employed were in the ranges 1.5 to 1.8 mg/ml and 0.30 to 0.35 mg/ml in the near UV and far UV respectively. The scan rate and time constant were 10 nm/min and 2 s respectively and the spectra shown were the average of three scans. The samples of PKB had been transferred to a buffer with NaF replacing NaCl in order to minimize problems caused by the high absorbance of chloride ions below 200 nm.

RESULTS AND DISCUSSION

Atomic resolution PKBαPH-Ins(1,3,4,5)P_4 structure

The atomic resolution (0.98 Å) structure of the native human PKBαPH domain in complex with Ins(1,3,4,5)P_4 was solved by molecular replacement using the previously characterized 1.4 Å selenomethionine-PKBαPH-Ins(1,3,4,5)P_4 complex structure [22] as a starting model (Figure 1, upper panel). As expected, the native PKBαPH-domain structure was virtually identical to the selenomethionine PKBαPH structure [root-mean-square deviation (RMSD) on all atoms of 0.07 Å]. It possesses the standard PH-domain fold [6], with seven β-strands forming two orthogonal anti-parallel β-sheets, closed at one end by the C-terminal α-helix (Figure 1). At the other end of the β-barrel lie three loops (VL1–VL3), that are variable, both in sequence and length, in all known PH domains [5,6] (Figure 1). In the case of PKBαPH, these loops form a highly basic pocket into which the head groups of PtdIns(3,4,5)P_3 and PtdIns(3,4)P_2 can bind (Figure 2). The main interactions were shown previously to be mediated through binding to the 3- and 4-phosphates, whereas the 5-phosphate makes no significant interactions, thus explaining why PKB binds both PtdIns(3,4,5)P_3 and PtdIns(3,4)P_2 with similar affinity [22] (Figures 1 and 2). At the atomic resolution presented here, density was observed for some of the axial hydrogen atoms on the Ins(1,3,4,5)P_4 molecule (Figure 2, upper panel) and for some of the protein hydrogens.

We have described previously a direct comparision of the PH domain structure of PKBαPH-Ins(1,3,4,5)P_4 with other PH domains crystallized in complex with Ins(1,3,4,5)P_4 [22]. Similarly, the present atomic resolution complex shows that the orientation of the Ins(1,3,4,5)P_4 ligand within the binding site of PKBαPH is different from the orientation of this ligand in DAPP1, GRP1 or BTK [33–35]. Despite the D2 hydroxy group of the PKBαPH-Ins(1,3,4,5)P_4 structure facing into the protein, as with the structures of DAPP1, GRP1 and BTK, the inositol ring in the PKBαPH-Ins(1,3,4,5)P_4 structure is rotated approximately 45° about the ring, and the ring as a whole is shifted 4 Å towards the core of the protein [22].

Comparison of the PKBαPH apo structure and the PKBαPH-Ins(1,3,4,5)P_4 complex

The 1.65 Å apo PKBαPH domain structure was solved by molecular replacement using the previously characterized selenomethionine PKBαPH-Ins(1,3,4,5)P_4 structure [22] (Figure 1). This also possesses the standard PH domain fold, however, there are significant differences between the conformation of the apo structure and the Ins(1,3,4,5)P_4 complex with an RMSD of 0.95 Å on all Cα atoms after superposition (Figures 1 and 2). Firstly analysis of the ligand-binding pocket in the apo PKBαPH domain structure shows it to be occupied by a complex hydrogen bonding network centred around ionic interactions between Arg-86, Lys-14, Glu-17, and Asn-53, as well as several water molecules (Figure 2, middle panel). This network of hydrogen bonds is disrupted upon Ins(1,3,4,5)P_4 binding, resulting in Arg-86 moving 2.3 Å towards the 4-phosphate and Lys-14 moving 1.2 Å to bind the 3- and 4-phosphates (Figure 2, upper panel). Asn-53, which binds to the 3- and 4-phosphates in the Ins(1,3,4,5)P_4 complex, makes three hydrogen bonds with water molecules in the apo

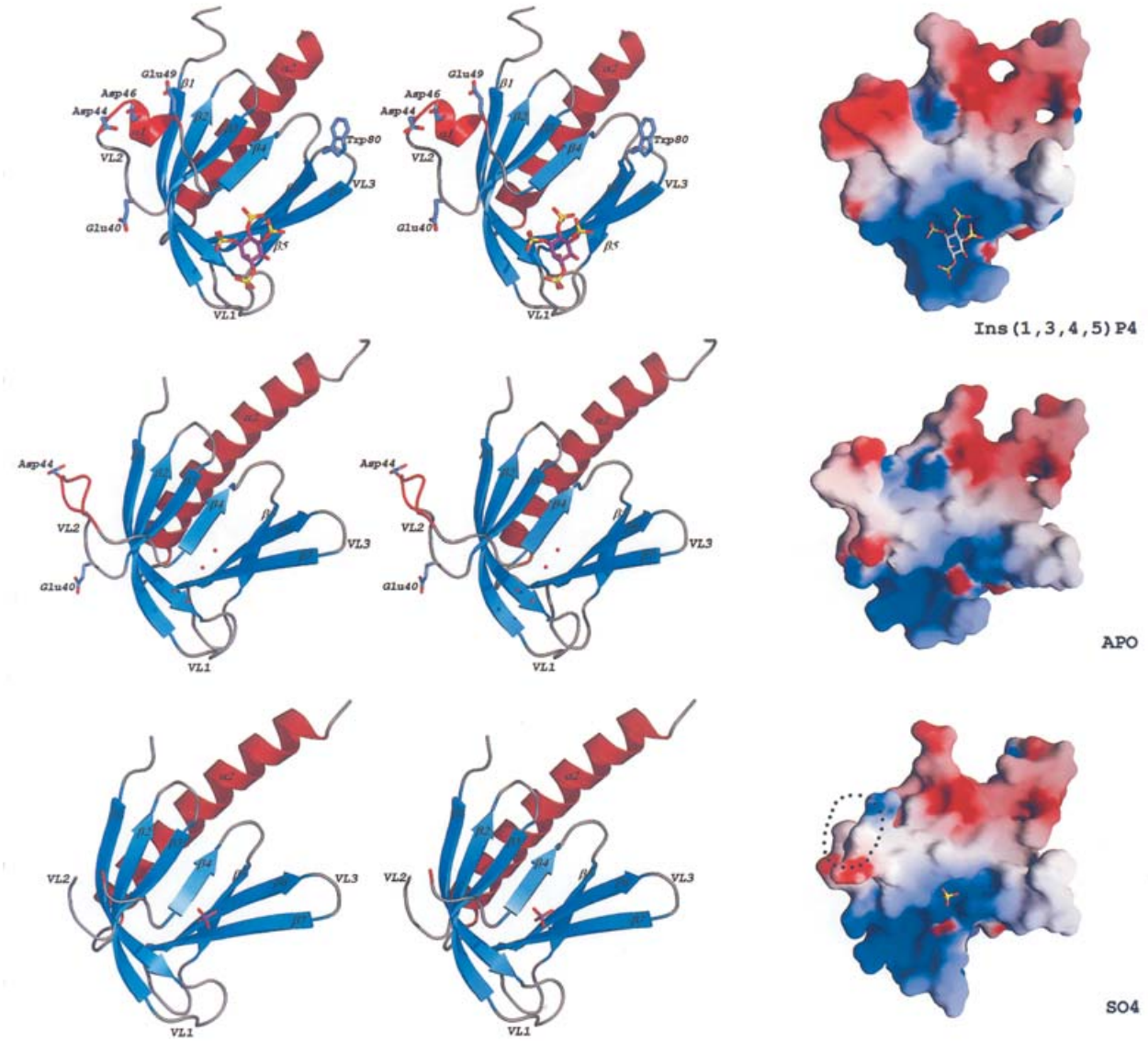

Figure 1 Overview of the PKBαPH apo and complex structures

For each of the structures, the protein is shown as a ribbon drawing, with the seven β-strands (labelled β1–β7) shown in blue and the α-helices (labelled α1–α2) shown in red. The negatively charged residues on loop VL2 and the exposed Trp-80 are shown with grey/blue carbons. The region of VL2 showing most change between the apo and complex structures is shown with red alpha carbons. Ins(1,3,4,5)P_4 (top panel) and the sulphate (labelled 'SO4', bottom panel) are shown as sticks models. In the apo structure ('APO', middle panel), key water molecules are indicated by red spots. On the right hand side, the electrostatic surface potential (calculated with GRASP [32]) is shown for each of the structures. Blue areas (+ 6kT) represent highly positively charged residues, red areas (− 6kT) indicated highly negatively charged residues. The absence of VL2 in the sulphate-containing apo structure is shown by a ring of black dots surrounding the area where the loop should be located when compared with the complex structures.

PKBαPH domain structure (Figure 2, middle panel). Asn-53 is in a similar position in both the apo structure and the Ins(1,3,4,5)P_4 complex. Interestingly, the acidic Glu-17 is repelled from the ligand-binding site by the negatively charged phosphoinositide, resulting in a conformational change of VL1 (residues 15–22), with backbone shifts up to 2.5 Å at Tyr-18 (Figure 2). In addition, the Tyr-18 side chain moves 5.0 Å away from the binding pocket to create space for the 5-phosphate of the Ins(1,3,4,5)P_4 molecule (Figure 2). If this movement did not occur there would be steric hindrance preventing accommodation of the 5-phosphate. Movement of Glu-17 away from the ligand-binding pocket could enable the movement of Arg-86 towards the 4-phosphate. Interaction of the PKBαPH domain with Ins(1,3,4,5)P_4 also results in Arg-23 moving 6.2 Å inwards to make contact with the 1- and 3-phosphates.

Another significant conformational change between the apo structure and Ins(1,3,4,5)P_4 complex is that the VL3 loop is positioned up to 7.4 Å away from the phosphoinositide-binding pocket in the apo structure compared to its position in the complex (Figure 1, upper and middle panels). This conformational change might be mediated by the movement of Arg-86 found at the base of VL3 towards the 4-phosphate upon Ins(1,3,4,5)P_4 binding. Unusually for a hydrophobic residue, Trp-80 found at the tip of VL3 is completely solvent-exposed in both the apo and complex

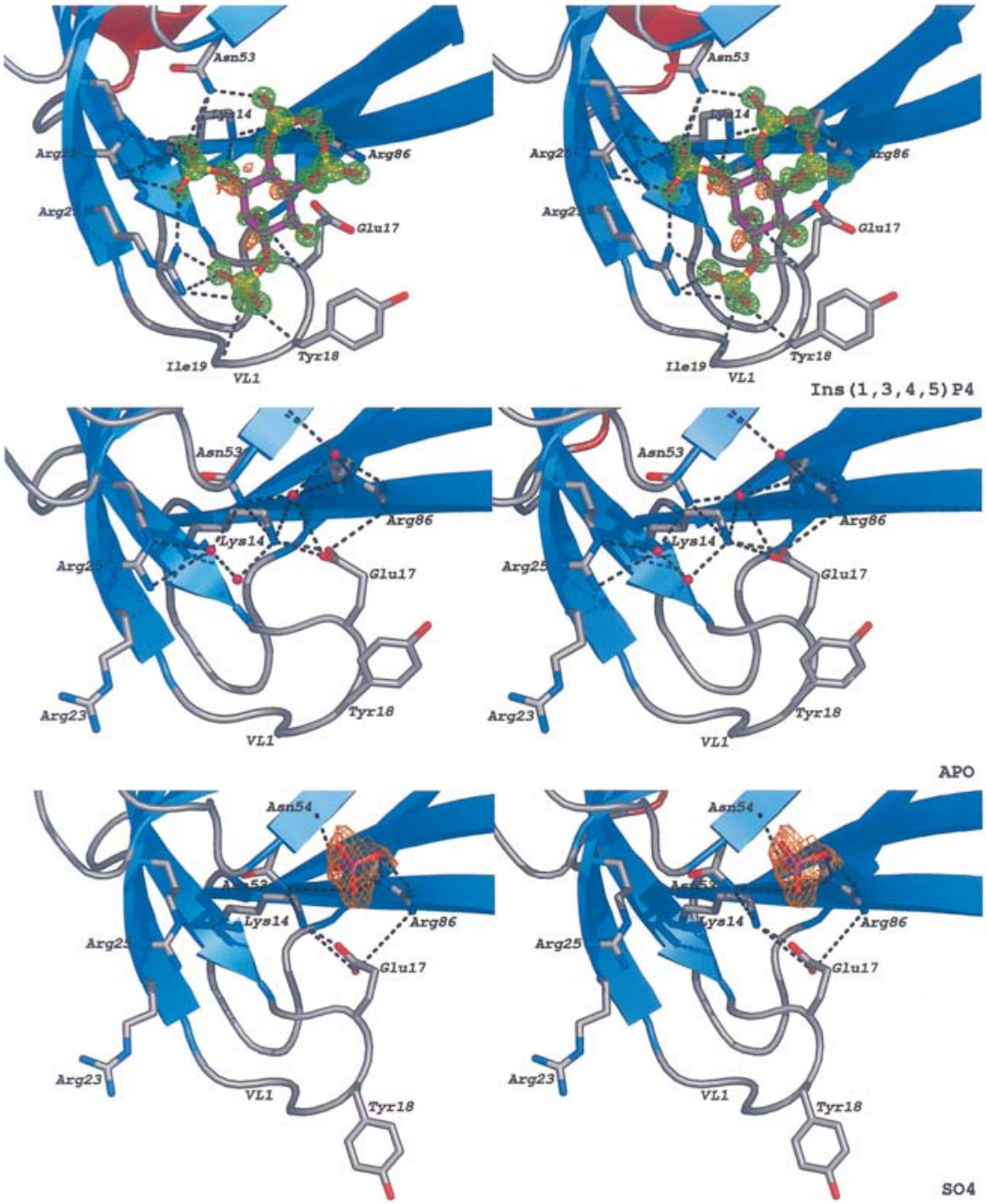

Figure 2 Details of the ligand-binding site

Ribbon drawing of the PKBαPH-binding site, for the apo structure and the Ins(1,3,4,5)P_4 and sulphate complexes, with colours as in Figure 1. The side chains of residues lining the binding pocket are shown as sticks with grey carbons. Ins(1,3,4,5)P_4 (top panel) and the sulphate (bottom panel) are shown as sticks models. In the apo structure (middle panel), key water molecules are indicated by red spheres. Hydrogen bonds between the molecules in the binding pocket and the protein are shown as broken black lines. $2|F_o|-|F_c|,\phi_{calc}$ density for Ins(1,3,4,5)P_4 before the inclusion of riding hydrogens, is shown as green mesh (top panel), contoured at 3.6 σ, while $|F_o|-|F_c|,\phi_{calc}$ density (contoured at 2.5 σ) for some of the axial hydrogens on the Ins(1,3,4,5)P_4 molecule and the sulphate ion, is shown as an orange mesh.

PKBαPH domain structures. The Trp-80 side chain is possibly mobile as judged by the lack of well-defined electron density. The presence of a solvent-exposed hydrophobic residue suggests that this region could potentially form a region of interaction to either the remainder of the PKB sequence or to one of the other PKB interacting proteins that have been suggested to bind to the PH domain of PKB [36].

The most dramatic conformational change between the apo and complex PKBαPH domains, is the absence of the short acidic α-helix of VL2 in the apo structure (Figure 1, middle panel). In the apo structure, the VL2 loop is not well defined by the electron density maps, suggesting that in the apo form this loop is flexible. However, sufficient density can be seen in the 1.65 Å dataset to trace the VL2 backbone. VL2 does not assume ordered secondary structure, such as the α-helix observed in the Ins(1,3,4,5)P_4 complex structure. To achieve the formation of the VL2 α-helix, this loop must undergo a 7.6 Å shift upon Ins(1,3,4,5)P_4 binding. A key result of this conformational change

is the clustering of the 3–4 negative charges (Asp-44, Asp-46, Glu-49 and to a lesser extent Glu-40), to form the acidic patch seen facing the solvent (Figure 1, upper panel).

It is possible that if VL2 or VL3 formed an intramolecular interaction with the PKB kinase domain in the absence of 3-phosphoinositides, upon lipid binding, the large conformational changes identified in these regions of the PH domain of PKBα could result in the exposure of the activation loop of PKBα kinase domain, allowing PDK1 to phosphorylate and hence activate PKB. In this respect Bellacosa et al. [37] reported that mutation of Glu-40 (at the base of VL2) to a lysine residue increased the activity of PKBα 2–3-fold in unstimulated and wortmannin-treated cells, and also showed *in vitro* that PDK1 was able to phosphorylate this mutant more efficiently at lower concentrations of PtdIns(3,4,5)P_3 *in vitro* than wild-type PKB. The authors of this study [37] interpreted their results as indicating that the PKBα (Glu-40 $\rightarrow$ Lys) mutant interacted with higher affinity with PtdIns (3,4,5)P_3. However, as Glu-40 is not located in the Ins(1,3,4,5)P_4-binding site, an alternative explanation is that in the PKBα (Glu-40 $\rightarrow$ Lys) mutant, the VL2 region of the PKBαPH domain could be less able to interact with the PKB kinase domain, thereby promoting the ability of PDK1 to phosphorylate Thr-308 efficiently in the presence of lower concentrations of PtdIns (3,4,5)P_3.

It is worth noting that the ligand-induced conformational changes described here appear to be unique to PKBα, compared with other PH domains for which structures are available in the presence and absence of Ins(1,3,4,5)P_4 [33–35,38]. The conformational changes in these PH domains are limited to movement of VL1 to accomodate the D5 phosphate groups and, in the case of DAPP1 [33], movement of the loop between the β5 and β6 strands. The role of the PKBαPH domain in the regulation of PKBα activation by PDK1 is, so far, a unique role for a PH domain, and it is therefore not surprising that such large conformational changes are not observed in other PH domains.

PKBαPH-sulphate complex structure

Upon solution and refinement of a 1.25 Å PKBαPH dataset (see Experimental procedures and Table 1), it became apparent that in this structure the ligand-binding pocket contained an ordered sulphate molecule rather than the expected diC$_8$-PtdIns(3,4,5)P_3 molecule.

Comparison of this structure with both the apo structure and Ins(1,3,4,5)P_4 complex (Figures 1 and 2), shows that the sulphate molecule is located approximately 2.2 Å from the 4-phosphate of the Ins(1,3,4,5)P_4 molecule in the complex structure, and close to one of the water molecules in the apo structure that hydrogen-bonds to Arg-86 and Asn-54 (Figure 2). The sulphate molecule forms similar interactions as the 4-phosphate of Ins(1,3,4,5)P_4 molecule in the complex structure, including two hydrogen bonds to the side chain of Arg-86, and one to the side chain of Asn-53. The slight difference in location of the sulphate molecule compared with the 4-phosphate of the Ins(1,3,4,5)P_4 molecule, is likely to be due to the additional interactions that are made between the sulphate molecule and the backbone of Asn-54, as well as to the side chain of a symmetry-related Asn-31 backbone (Figure 2, bottom panel). The water-mediated hydrogen-bonding network in the lipid-binding pocket is significantly disrupted by the presence of the sulphate (Figure 2, bottom panel). However, the disruption of the hydrogen-bonding network is apparently not sufficient to induce the major conformational changes seen between apo and Ins(1,3,4,5)P_4 complex structures. Overall, the PKBαPH-sulphate structure resembles the apo structure (RMSD 0.28 Å on all Cα atoms) more closely than the PKBαPH-Ins (1,3,4,5)P_4 complex (RMSD 0.90 Å). The head group-binding residues (Tyr-18, Arg-23, Arg-86) as well as VL1 and VL3 are found at the same position in the PKBαPH-sulphate structure as in the PKBαPH apo structure (Figures 1 and 2, middle and bottom panels). It should be noted that in the PKBαPH-sulphate structure part of the VL2 loop is disordered, suggesting that it is more flexible than in the apo state and possesses no detectable secondary structure. However, the residues in VL2 that are defined, are in the PKBαPH apo position. Overall these results suggest that the displacement of the hydrogen-bonding network and water molecules, at least by a sulphate molecule, are not sufficient to cause conformational changes in VL2 and VL3, and hence the number and strength of interactions between the ligand and PKBαPH is likely to be important in mediating these conformational changes.

Examination of other PH-domain structures that contain sulphate or phosphate, such as GRP1 and DAPP1 [33,34], reveal 2 oxyanions in each structure bound at sites within 0.4–1.5 Å of the 3- and 4-phosphates respectively. The difference between the number and positioning of the charged molecules in these structures and PKBαPH is likely to be due to the overall difference in the positioning of the Ins(1,3,4,5)P_4 molecule in the PKBαPH domain [22] and that Ins(1,3,4,5)P_4 binding is required to induce conformational changes required to optimize the binding pocket to interact with its ligand.

CD spectroscopy

To investigate further the conformational changes seen in the crystal structures, we performed CD spectroscopy on PKBαPH. The far-UV CD spectrum of PKBαPH is unusual (Figure 3). In addition to the negative ellipticity in the range 225 to 205 nm and the positive ellipticity around 195 nm, which are characteristic of protein secondary structural features such as α-helix and β-sheet, there is a small positive peak at 232 nm, which is thought to reflect contributions made by tryptophan side chains located in β-strands [39,40]. Analysis of the far-UV CD spectrum was undertaken using the SELCON procedure [41]. The closest match from the protein database was with pepsin and the secondary structure composition was indicated to be α-helix 18%, anti-parallel β-sheet 25%, parallel β-sheet 6%, turn 20%, other 31%. These estimates should be compared with the PKBαPH X-ray structure that indicates that 20 (18%) and 51 (45%) of the 113 residues of PKB are located in α-helix and β-sheet elements respectively. Thus, the SELCON procedure gives a satisfactory α-helical content but is not able to account in detail for the high β-sheet content.

On addition of the ligand Ins(1,3,4,5)P_4, there is relatively little systematic change in the far-UV CD spectrum of wild-type PKB (Figure 3A); the maximum change in ellipticity over the range 230 to 200 nm is 8%. From these data it is not possible to conclude that there is a significant change in α-helix or β-sheet content on binding the ligand. However, it should be pointed out that the expected increase in helical content from comparison of the two structures would be small and that any increase in signal in the range 220 to 200 nm might be masked by changes in the contribution from the high β-sheet content of the structure.

In the near UV region (Figure 3B), however, there is evidence for an Ins(1,3,4,5)P_4-induced conformational change in the protein. Distinct changes are seen in all 4 peaks in the range from 300 to 282 nm. These changes would be consistent with the conformational changes that occur on ligand binding, as seen in the crystal structures described here, which show that the regions of the protein around Glu-17 and Arg-86 undergo structural changes.

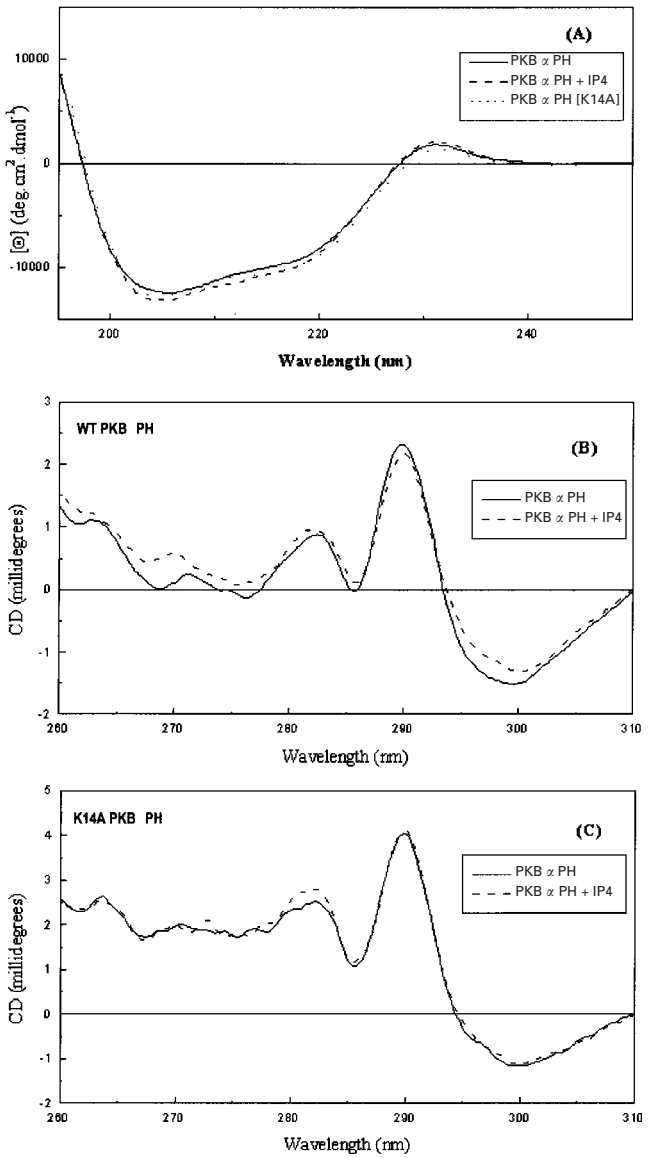

Figure 3 CD spectra of PKB

(**A**) The far-UV CD spectra of wild-type PKBαPH, wild-type PKBαPH plus 1.2 molar equivalents of Ins(1,3,4,5)P_4 (PKBαPH + IP4), and the mutant PKBαPH[K14A]. The spectrum of PKBαPH[K14A] plus 1.2 molar equivalents of Ins(1,3,4,5)P_4 is almost identical with that of PKBαPH[K14A]. Results are presented in molar ellipticity units, $[\theta]_M$. (**B**) The near-UV CD spectrum of wild-type PKB in the absence and presence (PKBαPH + IP4) of 1.2 molar equivalents of Ins(1,3,4,5)P_4. The protein concentration was 1.5 mg/ml. (**C**) Shows the near-UV CD spectrum of the K14A mutant of PKB in the absence (PKBαPH) and presence (PKBαPH + IP4) of 1.2 molar equivalents of Ins(1,3,4,5)P_4. The protein concentration was 1.8 mg/ml. In Panels (**B**) and (**C**) the data are represented in millidegree units.

These changes might be expected to affect neighbouring aromatic amino acid side chains including Tyr-18, Trp-22 and the unusually exposed Trp-80 insert of VL3. Thus the CD results support the proposal that the binding of the ligand Ins(1,3,4,5)P_4 leads to a conformational change in apo-PKBαPH.

As a control, the CD spectra of the PKBαPH[K14A] mutant [which does not interact with PtdIns(3,4,5)P_3] in the absence and presence of Ins(1,3,4,5)P_4 were also measured (Figure 3C). The spectra are similar to wild-type PKBαPH, showing no significant change in secondary structure content and indicating that PKBαPH[K14A] is properly folded. In addition, there was no detectable effect on the far-UV CD spectrum of the PKBα-PH[K14A] mutant following the addition of Ins(1,3,4,5)P_4 (results not shown). Addition of Ins(1,3,4,5)P_4 to the PKBα-PH[K14A] mutant also had no significant effect on the near-UV CD spectrum (Figure 3C). This provides further evidence that the changes observed in the CD spectrum following the binding of wild-type PKBαPH to Ins(1,3,4,5)P_4 arise from ligand-induced perturbation of its structure.

Conclusions

In this study we have provided the first direct structural evidence showing that the binding of PKBαPH to the lipid head group of PtdIns(3,4,5)P_3 results in significant conformational changes. These occur in the ligand-binding pocket of the PH domain, as well as in the VL2 and VL3 loops. To our knowledge this is the first report of a significant conformational change taking place in any PH domain induced by phosphoinositide binding. As discussed in the Introduction, there is considerable *in vitro* [18,19] and cellular [20,21] evidence that supports the notion that binding of full-length PKB to PtdIns(3,4,5)P_3 induces a conformational change that converts PKB into a substrate for PDK1, perhaps by exposing the activation loop Thr residue for phosphorylation. An important question is how this conformational change is transmitted to the kinase domain of PKB. We speculate that both VL2 and VL3 loops, which are removed from the ligand-binding pocket and would be predicted to be pointing away from the membrane surface, could potentially make contacts with the non-PH domain regions of PKB. Thus the VL2/VL3 loops are possible candidates for transmission of the phosphoinositide-binding signal to the catalytic region of PKB enabling subsequent phosphorylation of the activation loop by PDK1.

We thank the European Synchrotron Radiation Facility, Grenoble, for the time at beam lines ID29/ID14, the Daresbury Synchrotron Radiation Source for time and support on Station 14.2. We are grateful to Nick Morrice for performing MS analysis and to the DNA Sequencing Service, School of Life Sciences, and University of Dundee for DNA sequencing. C. C. M. is supported by a BBSRC CASE studentship, D. vA. by a Wellcome Trust Career Development Research Fellowship, D. R. A. by the Medical Research Council (UK), Diabetes UK, Association for International Cancer Research, and the pharmaceutical companies supporting the Division of Signal Transduction Therapy unit in Dundee (AstraZeneca, Boehringer Ingelheim, Novo-Nordisk, Pfizer, GlaxoSmithKline). The coordinates and structure factors have been deposited with the Protein Database {entries: 1UNP (apo), 1UNQ [Ins(1,3,4,5)P_4 complex], 1UNR (sulphate complex)}.

REFERENCES

1 Vanhaesebroeck, B., Leevers, S. J., Ahmadi, K., Timms, J., Katso, R., Driscoll, P. C., Woscholski, R., Parker, P. J. and Waterfield, M. D. (2001) Synthesis and function of 3-phosphorylated inositol lipids. Annu. Rev. Biochem. **70**, 535–602
2 Nakae, J., Park, B. C. and Accili, D. (1999) Insulin stimulates phosphorylation of the forkhead transcription factor FKHR on serine 253 through wortmannin sensitive pathway. J. Biol. Chem. **274**, 15982–15985
3 Lawlor, M. A. and Alessi, D. R. (2001) PKB/Akt: a key mediator of cell proliferation, survival and insulin responses? J. Cell Sci. **114**, 2903–2910
4 Cantley, L. C. (2002) The phosphoinositide 3-kinase pathway. Science (Washington, D.C.) **296**, 1655–1657
5 Isakoff, S. J., Cardozo, T., Andreev, J., Li, Z., Ferguson, K. M., Abagyan, R., Lemmon, M. A., Aronheim, A. and Skolnik, E. Y. (1998) Identification and analysis of PH domain-containing targets of phosphatidylinositol 3-kinase using a novel *in vivo* assay in yeast. EMBO J. **17**, 5374–5387
6 Lemmon, M. A. and Ferguson, K. M. (2000) Signal-dependent membrane targeting by pleckstrin homology (PH) domains. Biochem. J. **350**, 1–18
7 Scheid, M. P. and Woodgett, J. R. (2001) PKB/Akt: Functional insights from genetic models. Nat. Rev. Mol. Cell Biol. **2**, 760–768
8 Brazil, D. P. and Hemmings, B. A. (2001) Ten years of protein kinase B signalling: a hard Akt to follow. Trends Biochem. Sci. **26**, 657–664

9 Hill, M. M. and Hemmings, B. A. (2002) Inhibition of protein kinase B/Akt: implications for cancer therapy. Pharmacol. Ther. **93**, 243–251
10 Vivanco, I. and Sawyers, C. L. (2002) The phosphatidylinositol 3-kinase-Akt pathway in human cancer. Nat. Rev. Cancer **2**, 489–501
11 Testa, J. R. and Bellacosa, A. (2001) Commentary – Akt plays a central role in tumorigenesis. Proc. Natl. Acad. Sci. U.S.A. **98**, 10983–10985
12 Frech, M., Andjelkovic, M., Ingley, E., Reddy, K. K., Falck, J. R. and Hemmings, B. A. (1997) High affinity binding of inositol phosphates and phosphoinositides to the pleckstrin homology domain of RAC protein kinase B and their influence on kinase activity. J. Biol. Chem. **272**, 8474–8481
13 James, S. R., Downes, C. P., Gigg, R., Grove, S. J. A., Holmes, A. B. and Alessi, D. R. (1996) Specific binding of the Akt-1 protein kinase to phosphatidylinositol 3,4,5-trisphosphate without subsequent activation. Biochem. J. **315**, 709–713
14 Andjelkovic, M., Alessi, D. R., Meier, R., Fernandez, A., Lamb, N. J. C., Frech, M., Cron, P., Cohen, P., Lucocq, J. M. and Hemmings, B. A. (1997) Role of translocation in the activation and function of protein kinase. J. Biol. Chem. **272**, 31515–31524
15 Watton, S. J. and Downward, J. (1999) Akt/PKB localisation and 3-phosphoinositide generation at sites of epithelial cell-matrix and cell-cell interaction. Curr. Biol. **9**, 433–436
16 Alessi, D. R. (2001) Discovery of PDKI, one of the missing links in insulin signal transduction. Biochem. Soc. Trans. **29**, 1–14
17 Alessi, D. R. and Cohen, P. (1998) Mechanism of activation and function of protein kinase B. Curr. Opin. Genet. Dev. **8**, 55–62
18 Alessi, D. R., Deak, M., Casamayor, A., Caudwell, F. B., Morrice, N., Norman, D. G., Gaffney, P., Reese, C. B., MacDougall, C. N., Harbison, D. et al. (1997) 3-phosphoinositide-dependent protein kinase-1 (PDK1): structural and functional homology with the *Drosophila* DSTPK61 kinase. Curr. Biol. **7**, 776–789
19 Stokoe, D., Stephens, L. R., Copeland, T., Gaffney, P. R. J., Reese, C. B., Painter, G. F., Holmes, A. B., McCormick, F. and Hawkins, P. T. (1997) Dual role of phosphatidyl-inositol-3,4,5-trisphosphate in the activation of protein kinase B. Science (Washington, D.C.) **277**, 567–570
20 Biondi, R. M., Kieloch, A., Currie, R. A., Deak, M. and Alessi, D. R. (2001) The PIF-binding pocket in PDK1 is essential for activation of S6K and SGK, but not PKB. EMBO J. **20**, 4380–4390
21 Calleja, V., Ameer-Beg, S. M., Vojnovic, B., Woscholski, R., Downward, J. and Larijani, B. (2003) Monitoring conformational changes of proteins in cells by fluorescence lifetime imaging microscopy. Biochem. J. **372**, 33–40
22 Thomas, C. C., Deak, M., Alessi, D. R. and van Aalten, D. M. F. (2002) High-resolution structure of the pleckstrin homology domain of protein kinase B/Akt bound to phosphatidylinositol (3,4,5)-trisphosphate. Curr. Biol. **12**, 1256–1262
23 Yang, J., Cron, P., Thompson, V., Good, V. M., Hess, D., Hemmings, B. A. and Barford, D. (2002) Molecular mechanism for the regulation of protein kinase B/Akt by hydrophobic motif phosphorylation. Mol. Cell **9**, 1227–1240
24 Yang, J., Cron, P., Good, V. M., Thompson, V., Hemmings, B. A. and Barford, D. (2002) Crystal structure of an activated Akt/protein kinase B ternary complex with GSK3-peptide and AMP-PNP. Nat. Struct. Biol. **9**, 940–944
25 Otwinowski, Z. and Minor, W. (1997) Processing of X-ray diffraction data collected in oscillation mode. Methods Enzymol. **276**, 307–326
26 Navaza, J. (1994) AMoRe: an automated package for molecular replacement. Acta Cryst. A **50**, 157–163
27 Perrakis, A., Morris, R. and Lamzin, V. S. (1999) Automated protein model building combined with iterative structure refinement. Nature Struct. Biol. **6**, 458–463
28 Jones, T. A., Zou, J. Y., Cowan, S. W. and Kjeldgaard, M. (1991) Improved methods for building protein models in electron density maps and the location of errors in these models. Acta Cryst. A **47**, 110–119
29 Brunger, A. T., Adams, P. D., Clore, G. M., Gros, P., Grosse-Kunstleve, R. W., Jiang, J.-S., Kuszewski, J., Nilges, M., Pannu, N. S., Read, R. J. et al. (1998) Crystallography and NMR system: A new software system for macromolecular structure determination. Acta Cryst. D **54**, 905–921
30 Sheldrick, G. M. and Schneider, T. R. (1997) SHELXL: High-resolution refinement. Methods Enzymol. **277**, 319–343
31 Vriend, G. (1990) WHAT IF: a molecular modeling and drug design program. J. Mol. Graph. **8**, 52–56
32 Nicholls, A., Sharp, K. and Honig, B. (1991) Protein folding and association – insights from the interfacial and thermodynamic properties of hydrocarbons. Proteins **11**, 281–296
33 Ferguson, K. M., Kavran, J. M., Sankaran, V. G., Fournier, E., Isakoff, S. J., Skolnik, E. Y. and Lemmon, M. A. (2000) Structural basis for discrimination of 3-phosphoinositides by pleckstrin homology domains. Mol. Cell **6**, 373–384
34 Lietzke, S. E., Bose, S., Cronin, T., Klarlund, J., Chawla, A., Czech, M. P. and Lambright, D. G. (2000) Structural basis of 3-phosphoinositide recognition by pleckstrin homology domains. Mol. Cell **6**, 385–394
35 Baraldi, E., Carugo, K. D., Hyvonen, M., Surdo, P. L., Riley, A. M., Potter, B. V., O'Brien, R., Ladbury, J. E. and Saraste, M. (1999) Structure of the PH domain from Bruton's tyrosine kinase in complex with inositol 1,3,4,5-tetrakisphosphate. Structure Fold Des. **7**, 449–460
36 Brazil, D. P., Park, J. and Hemmings, B. A. (2002) PKB binding proteins: Getting in on the Akt. Cell **111**, 293–303
37 Bellacosa, A., Chan, T. O., Ahmed, N. N., Datta, K., Malstrom, S., Stokoe, D., McCormick, F., Feng, J. N. and Tsichlis, P. (1998) Akt activation by growth factors is a multiple-step process: the role of the PH domain. Oncogene **17**, 313–325
38 Hyvonen, M. and Saraste, M. (1997) Structure of the PH domain and Btk motif from Bruton's tyrosine kinase: Molecular explanations for X-linked agammaglobulinaemia. EMBO J. **16**, 3396–3404
39 Kirkitadze, M. D., Henderson, C., Price, N. C., Kelly, S. M., Mullin, N. P., Parkinson, J., Dryden, D. T. F. and Barlow, P. N. (1999) Central modules of the vaccinia virus complement control protein are not in extensive contact. Biochem. J. **344**, 167–175
40 Freskgard, P. O., Martensson, L. G., Jonasson, P., Jonsson, B. H. and Carlsson, U. (1994) Assignment of the contribution of the tryptophan residues to the CD spectrum of human carbonic-anhydrase 2. Biochemistry **33**, 14281–14288
41 Sreerama, N. and Woody, R. W. (1993) A self-consistent method for the analysis of protein secondary structure from circular-dichroism. Anal. Biochem. **209**, 32–44

Received 13 August 2003/1 September 2003; accepted 10 September 2003
Published as BJ Immediate Publication 10 September 2003, DOI 10.1042/BJ20031229